18TH WORLD CONFERENCE ON EARTHQUAKE ENGINEERING
WCEE2024
MILAN

MILAN, ITALY
30TH JUNE - 5TH JULY 2024

www.wcee2024.it

PRE-TEST NUMERICAL MODELING OF THE CFS-NHERI 10-STORY CAPSTONE BUILDING

J. Zhang[1], A. Singh[2], M. Eladly[2], B. W. Schafer[2] & T. C. Hutchinson[1]

[1] University of California San Diego – Department of Structural Engineering, La Jolla, CA, USA, j-charlie-zhang@ucsd.edu

[2] Johns Hopkins University – Department of Civil and Systems Engineering, Baltimore, MD, USA

Abstract: *The use of cold-formed steel (CFS) framing for taller structures in the North American construction industry is limited within current codified guidelines, despite its robust structural performance as observed in shake table and component-level tests. To fully utilize this form of construction and meet the growing needs of urban housing, a full-scale 10-story CFS-framed building is planned to commence construction and preparation for shake table testing at the UC San Diego 6-DOF Large High-Performance Outdoor Shake Table (LHPOST6) in late summer 2024. This landmark test program will serve as the capstone effort to the Collaborative Research Program entitled: Seismic Resiliency of Repetitively Framed Mid-Rise Cold-Formed Steel Buildings (CFS-NHERI). Courtesy of the newly upgraded LHPOST6, this unique test program will provide an opportunity to investigate the system-level performance of tall CFS buildings under multi-directional seismic excitation.*

In preparation for the capstone test phase, two finite element (FE) models are under development, namely: model 1 is a design-level phenomenological-based model, while model 2 is a refined, stacked wall-line FE model, each undertaken using the OpenSeesPy framework. The aim of these models is to predict the dynamic characteristics and response of this 10-story test building under different intensities of earthquake input. Model 1, a design-level FE model, is developed using a strategy adopted to predict the response of a full-scale 6-story CFS building that was tested under unidirectional shaking. The robustness of this modeling approach has been evaluated and compared against prior test results and good agreement was observed. This simplistic strategy boasts efficiency in computing by minimizing model degrees-of-freedom, assuming rigid diaphragms, lumped masses, and uniaxial spring elements to capture the lumped behaviors of the lateral load resisting shear walls, gravity walls, and tie-down systems. Model 2 boasts higher fidelity, though requires parallel computing to enhance the computational speed, with wall lines captured with a suite of discrete beam and truss elements and interconnecting springs at boundary and other connections to capture local behaviors induced along the lateral force resisting system and associated boundaries. These numerical models will be cross-compared and used for pre-test analyses and to support selection and scaling of ground motions during the full-scale shake table program.

1. Introduction

1.1. Motivation and Prior Studies

Cold-formed steel (CFS) framing solutions have gained popularity in the North American construction industry particularly in use of low-rise and mid-rise buildings. However, existing building codes (ASCE/SEI 2016, 2022) currently restrict the use of CFS framing for taller structures to a maximum height of 19.8 m (65 ft). Extensive research conducted on various components of CFS buildings has contributed significantly to the advancement of codes and standards in the CFS field such as AISI S100 (2016), S240 (2015a), and S400 (2015b), and enhanced the understanding of the behavior of CFS framing components. Yet, investigation of the overall

system-level performance of cold-formed steel buildings under earthquake excitation has remained limited. To the best of the authors' knowledge, only two projects thus far have investigated the system-level seismic performance using large shake tables in Northern America. Peterman et al. (2016) conducted shake table testing on a full-scale two-story CFS-framed building, namely the CFS-NEES project, at the NEES@Buffalo site, marking the first such tests to investigate the system-level response of a CFS-framed building in North America. The CFS-NEES test building had a floor plan dimension of 15.2 m x 7 m (49 ft and 9 in x 23 ft). Hutchinson et al. (2021) performed seismic testing and post-earthquake fire testing of a mid-rise full-scale 6-story CFS wall-braced building, referred to as the CFS-HUD project. These tests were conducted at the NEES@UC San Diego site. The CFS-HUD test building featured a uniform floor plan with a dimension of 10.4 m x 7.3 m (34 ft x 24 ft) and a story height of 3.1 m (10 ft).

1.2. CFS-NHERI 10-story building specimen

The multi-university-industry project entitled: Seismic Resiliency of Repetitively Framed Mid-Rise Cold-Formed Steel Buildings, funded through the National Science Foundation (NSF), referred to as CFS-NHERI, was undertaken to advance knowledge of the seismic performance of mid-rise CFS-framed building systems. The project sought to leverage this knowledge to support improvements in the seismic design codes for such systems. Thus far within the CFS-NHERI project, a set of experiments have been conducted to gain insights into the nonlinearities at the component and connection levels. Singh et al. (2022b, 2022c) tested wall line assemblies with various configurations utilizing shake table and quasi-static testing. Specimen details include unfinished or finished, symmetrical or unsymmetrical, Type I or Type II shear wall detailing configurations, tension tie rods or holdowns as anchorage detailing, and presence of window openings. Notably, the application of finish on the exterior wall line was found to significantly increase the lateral strength and stiffness of the wall line. Zhang et al. (2021, 2022b) conducted connection tests to investigate the screw connection behavior to support the use of steel sheet sheathing with HSS sections. Castaneda (2022) tested floor diaphragm assemblies using CFS joists and various panels to characterize the lateral performance of such floor systems at the component level. The system-level tests will build on the learnings from these connection- and component-level tests performed within the CFS-NHERI project as serve as a capstone contribution. This unique tall CFS building will incorporate the use of prefabricated CFS wall lines and floor diaphragms for rapid construction at the test site.

A 10-story CFS-framed building is scheduled for construction and testing atop the newly upgraded 6-DOF Large High-Performance Outdoor Shake Table Facility (LHPOST6) at NHERI@UC San Diego Experimental Facility (Van Den Einde et al. 2021), presently to commence in late Summer 2024. This capstone experimental program will also provide a unique opportunity to evaluate the post-earthquake fire performance of the earthquake-damaged building. Notably unique to this tall building will be the integration of complete architectural finishes and a building height exceeding the height limitation set by current US design standards (ASCE/SEI 2016, 2022). The experiments will provide vital full-scale system-level benchmark test data for a state-of-the-art CFS building under multi-directional seismic input leading to seismic design codes improvements. Complimentary live fire tests lead by Cal Poly San Luis Obispo will facilitate additional understanding of the thermal and smoke spread within seismically damaged compartments. Additional information regarding the building test program may be found at https://cfs10.ucsd.edu/ (UC San Diego 2023).

The 10-story test building was designed as a CFS-framed building at a hypothetical location in a highly seismic region near Irvine, California with a corresponding Site Class C (very dense soil and soft rock) condition (Singh et al. 2022a). The following design parameters were assumed in accordance with ASCE 7-16: Risk Category: II, spectral acceleration at short periods, S_S = 1.261 *g*, spectral acceleration at a period of 1 second, S_1 = 0.452 *g*, and design spectral accelerations, S_{DS} = 1.009 *g* and S_{D1} = 0.452 *g*. The test building is constructed of all steel CFS studs, CFS-steel sheathed shear walls, gypsum-board-sheathed gravity walls, an exterior face with stucco on the north side, and a ledger-framed CFS diaphragm with cement panel. The lateral force resisting system of the test building consists of Type I shear walls featuring single-sided steel sheet sheathing and ledger framing for floor-to-wall connections. The structure was designed to have a total building height of 30.5 m (100 ft), which exceeds the height limitation of 19.8 m (65 ft) set by the current ASCE 7-16 and 7-22 design standards. The design effective seismic weight, *W* of the building was estimated as 1575.0 kN (354.1 kips) and the design seismic base shear force, *V* was calculated as 173.2 kN (38.9 kips) in both orthogonal directions. Singh et al. (2022a) summarized the structural design narrative of the test building and provided additional details. Singh et al. (2024) provides additional design updates regarding the egress system, the

addition of a resilient modular stairs tower with drift-release connections. Figure 1a provides a 3D rendering of the proposed CFS-NHERI building specimen on top of the LHPOST6.

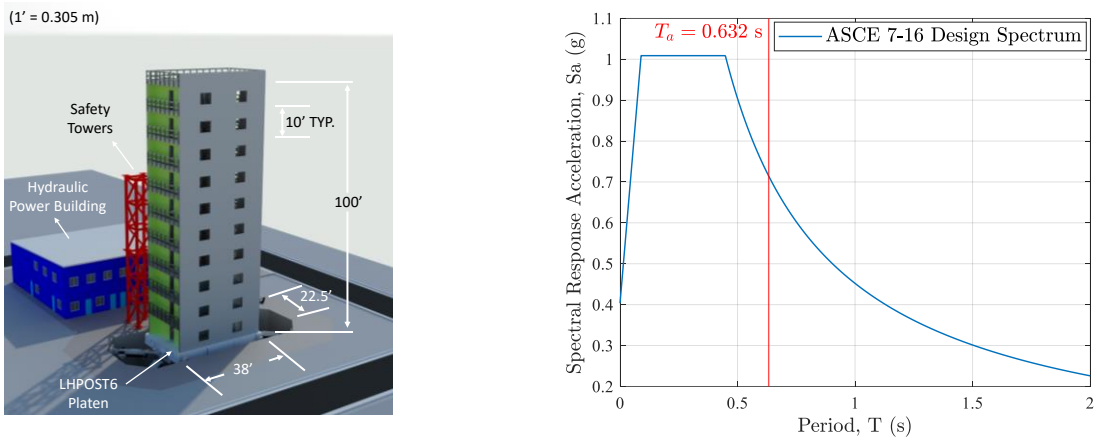

(a) (b)

Figure 1. (a) Rendering of CFS-NHERI 10-story test building atop LHPOST6 (view from northeast) and (b) design spectrum of the CFS-NHERI 10-story test building

1.3. Design-level building period and site-specific spectrum

The approximate fundamental period (T_a) that was used for design purposes was determined from the equation as Eq. (1) per ASCE 7-16:

$$T_a = C_t h_n^x \quad (1)$$

where h_n is the structural height (100 ft) and the coefficients C_t and x are determined as 0.02 and 0.75. Therefore, the approximate fundamental period of the test building was determined as 0.632 s for both the E-W and the N-S directions. Figure 1b shows the design spectrum of the test building, based on the selected site with overlay of the ASCE 7 estimated fundamental period.

1.4. Modeling approaches adopted in CFS wall-braced and similar structural systems

Three-dimensional structural analysis models are essential to simulate the behavior of building systems under varying loading conditions, especially at the pre-test planning stage of this benchmark test. The level of modeling detail greatly affects the required computational resources. This section will provide a brief review of modeling approaches that have been explored for the system-level performance of CFS structures and similar structural systems.

CFS wall-braced buildings

Leng et al. (2017) developed high-fidelity computational models for a 2-story cold-formed steel framed building with oriented strand board (OSB) sheathed shear walls (CFS-NEES test building) in OpenSees (McKenna 2000) that featured explicit modeling of shear walls, holddowns, and gravity wall. These models were validated against the measured response at different phases of the test building. Franklin et al. (2019) proposed an efficient modeling method for the same test building in ETABS for elastic analysis that featured the use of an equivalent shear modulus shell element for shear walls and gravity walls and demonstrated good accuracy when compared with the test results. Similarly, Campiche et al. (2020) developed computationally efficient models that considered varying modeling cases (without or with gravity walls and without or with finishes) in OpenSees, compared the models against the shake table testing results of a 2-story gypsum-sheathed CFS building, and achieved acceptable predictions. Most recently, Singh (2023) developed an OpenSees finite element model for a 6-story CFS-framed building (CFS-HUD test building) that featured the modeling of shear walls, gravity walls as nonlinear shear springs, and the modeling of continuous tie-rod systems. Good agreement between the numerical model predictions and experiment results was observed and this modeling approach therefore serves as the basis for future development in predictive tools for the prediction of seismic response of mid-rise CFS-framed buildings.

Wood shear wall-braced buildings

Buildings with lateral force resisted courtesy of wood shear wall-bracing have many of the same conceptual detailing characteristics of CFS wall-braced systems. In this regard, previous modelling efforts for these systems are equally valuable. Folz and Filiatrault (2004a, 2004b) developed a simple numerical model to predict the dynamic characteristic, quasi-static pushover, and seismic response of the woodframe test building featured in the CUREE-Caltech Woodframe Project. This model was composed of rigid horizontal diaphragms and nonlinear shear spring elements representing the lateral load resisting shear walls. The predictive capabilities of the model were then compared with experimental results and shown to provide reasonably accurate estimates of the response. Following a similar approach, van de Lindt et al. (2010) developed a SAPWood model as part of the NEESWood Project. Predictions generated by the SAPWood model were compared against the experimental seismic responses of a full-scale two-story light-frame wood townhouse building and a substantial level of agreement was observed. In these projects and other efforts with the woodframe research contributions, pancake models developed were also identified as valuable tools due to their fast computational time and minimal demand on computational resources. Consequently, these models may be useful tools for practicing engineers and researchers for seismic analysis and design of such building systems.

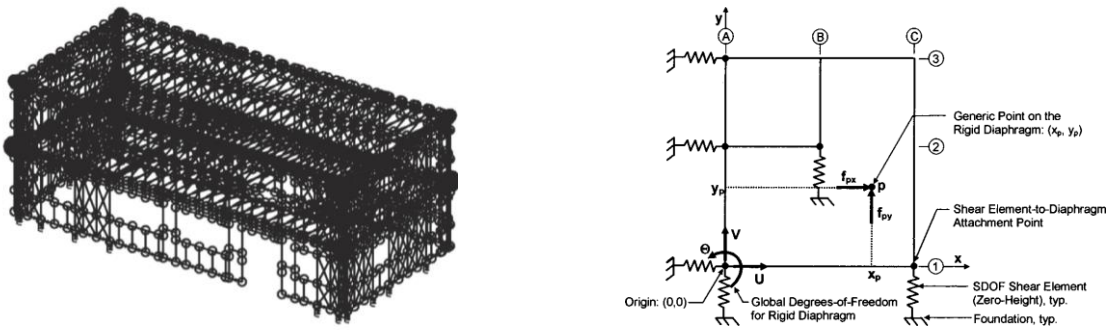

(a) (b)

Figure 2. Numerical models for (a) CFS-NEES test building (Leng et al. 2017); (b) single-story woodframe structure (Folz and Filiatrault 2004a)

2. Model 1: Design-level phenomenological-based approach

2.1. Model description

Model 1 is a design-level phenomenological-based model developed using the OpenSeesPy framework (McKenna et al. 2000, Zhu et al. 2018). The term design-level is suggested here, as the intent is to develop a model that is low in DOF, and simple in terms of capturing the detailing features of a building that most significantly contribute to its seismic response. As a result, model 1 is envisioned to be useful for pursuing numerous analyses runs on a desktop computer with reasonable efficiency (less than a day). Herein, the design-level FE model is developed using a strategy (Singh 2023) adopted to predict the response of a full-scale 6-story CFS building that was tested under unidirectional shaking (Hutchinson et al. 2021). The robustness of the model by Singh (2023) has been evaluated and compared against prior test results and good agreement was observed.

As noted, the CFS-NHERI 10-story test building has a uniform floor plan of 11.6 m x 6.9 m (38 ft x 22.5 ft) and a consistent 3.05 m (10 ft) story height. For this model, only gridline-to-gridline distance is considered and the contribution of the gravity wall (0.3 m or 1 ft) at each end along lines 1 and 2 is ignored. Therefore, the overall dimension will be 36 ft x 22 ft (11.0 m x 6.7 m). Figure 3 provides a schematic plan view of model 1. The test building is designed to have four 1.83 m (6 ft) shear walls in the longitudinal direction (along lines 1 and 2) and six 1.83 m (6 ft) shear walls in the transverse direction (along lines C, D, and E). It should be noted that the shear walls in the two orthogonal directions incorporate different tie-down detailing systems to represent the possible options reflecting regional preferences. The shear walls along lines C, D, and E adopt tension tie-rods between compression chord stud packs, while shear walls along lines 1 and 2 employ holdowns attached to chord stud packs. It is also worth noting that shear walls along lines 1 and 2 for levels 1-5 are detailed to resist much larger lateral forces, thus the chord studs are designed as hot-rolled steel HSS sections. Detailed

descriptions can be found in Singh et al. (2022a, 2024). The plan view shown in Figure 3 is stacked 10 times to comprise a 3D FEM model with wall lines modeled as shown in Figures 4 and 5.

As shown in Figures 4 and 5, the force-displacement behavior of shear walls is modeled as zero-length elements with Pinching4 uniaxial material property (Lowes et al. 2003). The connection to the foundation is modeled as a pin connection. A zero-length element with no rotational stiffness is used to provide a similar pin connection between adjacent floors. All nodes at the floor elevations are connected through *elasticBeamColumn* elements with high stiffness. Two *elasticBeamColumn* elements with high stiffness, whose length is half of the story height, connect the shear wall zero-length element to the node at floor elevations and to the node to which the zero-length "pin" element connects. A similar modeling approach is also adopted for the gravity wall, where the entire gravity wall between the shear walls (excluding openings) is lumped into one zero-length element with Pinching4 material property.

Modeling of the tie-down systems is proceeded slightly different depending on the types of tie-down systems as shown in Figures 4 and 5. For wall lines along lines 1 and 2 where holddowns are employed (Figure 4), each holdown is modeled as zero-length elements that consist of two zero-length springs in parallel: one spring for tension with an elastic-perfectly plastic (*ElasticPP*) material property and one spring for compression with an elastic-perfectly plastic gap (*ElasticPPGap*) material property. The length of the *elasticBeamColumn* element that connects the holdown is the full story height. For wall lines along lines C, D, and E where tie-rod systems are adopted (Figure 5), a vertical zero-length element at story mid-height is used to represent the vertical stiffness of the combined tie-rod and compression stud pack assembly. A simplified multi-linear elastic uniaxial material property will be assigned to this zero-length element (Singh 2023). Two *elasticBeamColumn* elements with high stiffness connect the zero-length element similarly to how they connect the shear wall zero-length element.

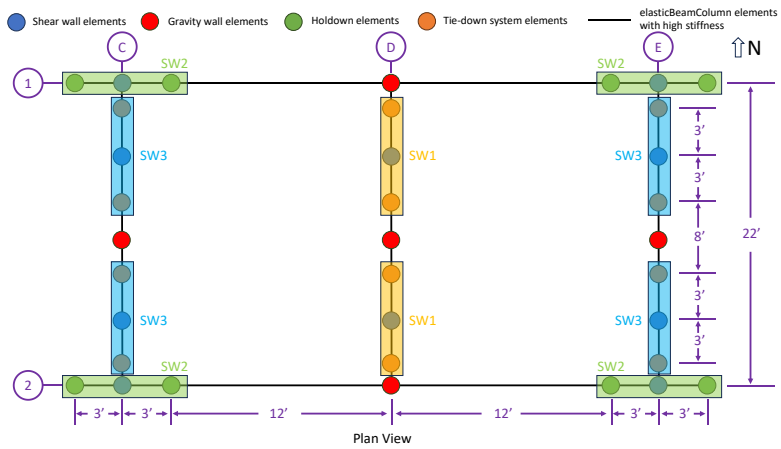

Figure 3. Schematic plan view of model 1

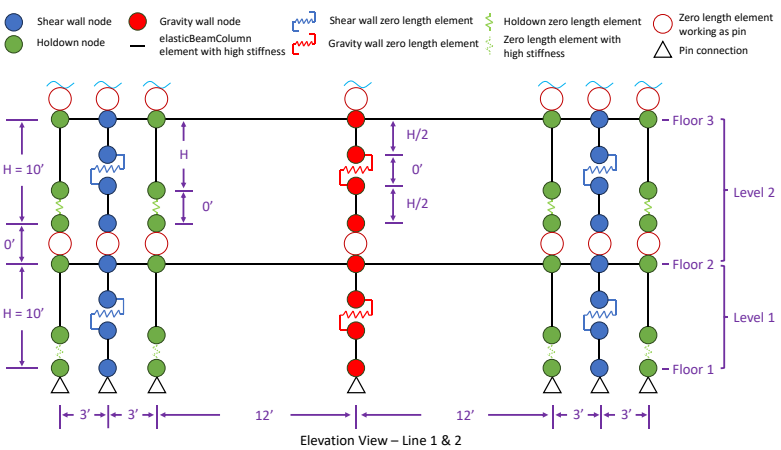

Figure 4. Schematic elevation view of wall lines 1& 2 of model 1

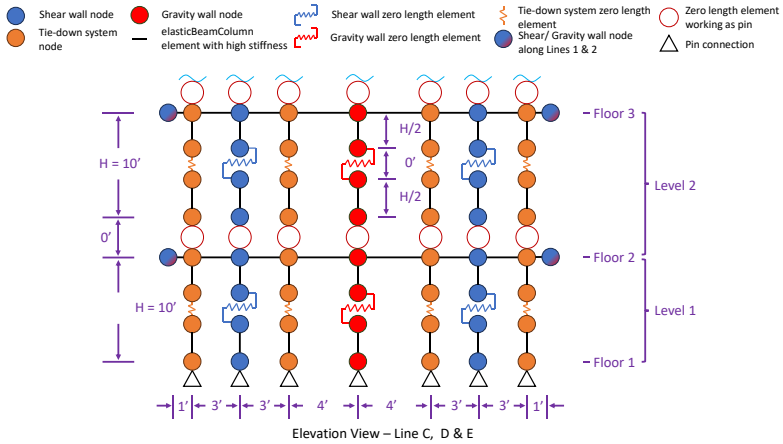

Figure 5. Schematic elevation view of wall lines C, D & E of model 1

Rigid diaphragms are employed for this model, with the seismic mass assumed lumped at the center of mass of the individual floors. Even though there is a stairs tower that will be in the west room, it is assumed that through the drift-release connections at mid-landing levels (see Singh et al. (2024)), the stairs will not contribute any stiffness to the overall stiffness of the building. Moreover, the system will entirely support its own gravity load.

2.2. Material properties of the various model 1 key components

Determination of the shear spring material properties, for the shear wall elements are characterized using the *Pinching4* material and utilizing test results by Rizk and Rogers (2017). These experiments involved monotonic and cyclic loading of 28 specimens with 14 configurations to determine the influence of the framing thickness on the performance of the shear walls. Calibration for the *Pinching4* material properties was performed based on test results from W1, W2, W7, W8, W9 and W10. For walls that are not designed using the test results from the Rizk and Rogers study, backbone curves that are available on the CFS shear wall database (Zhang et al. 2022a) are utilized. In addition, the lower floors of the CFS-NHERI building will utilize HSS chord studs, thus findings from Zhang (2023) using high fidelity ABAQUS FEM of CFS shear walls with HSS chord studs were adopted; notably indicating an observed strength increase of 2.7 over conventional stud packs. This value is adopted for shear wall shear spring properties for levels where HSS is utilized (namely levels 1-5). Subsequently, the backbone curves are scaled based on geometric properties, namely the W-series walls were 4’ x 8’, while the CFS-NHERI 10-story walls are 6’ by 10’. Singh et al. (2022c) quantified the additional strength from finish application as 9.3 kN/m (635 lb/ft) for an exterior EIFS layer and 5.4 kN/m (370 lb/ft) for an interior gypsum panel layer. Those values are employed to account for the additional strength increase due to the presence of finishes to the shear walls. Figure 6 presents two examples of the backbone curves for two of the shear walls used in the numerical model, noting the geometric scaling and strength increases adopted herein.

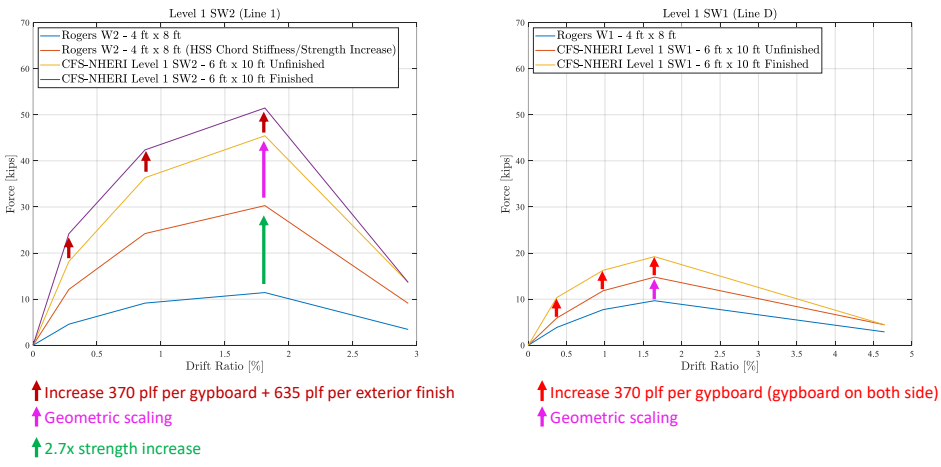

Figure 6. Examples of shear wall springs material properties

Figure 7 presents examples of the modeling assumption adopted to capture the behavior of the tie-down systems and holdowns properties, utilized in the N-S and E-W direction shearwalls, respectively. The tie-down system is modeled as an *ElasticMultilinear* zero-length element with properties calibrated from existing test data (Singh 2023) and scaled based on the geometric properties. The holdowns are modeled as two zero-length springs in parallel. The nominal strength for the *ElasticPP* materials is determined either by the test data for holdowns (ClarkDietrich 2023) or by the controlled nominal strength for holdown plates, in the latter case larger load requirements were needed at the lower floors (levels 2 to 7). For holdowns, the elastic stiffness is calculated using the ratio between the design load and the corresponding deflection at such load. For holdown plates, the elastic stiffness is then calculated using *EA/L* where *E* is the Young's Modulus for steel, *A* is the gross cross-sectional area, and *L* is the length.

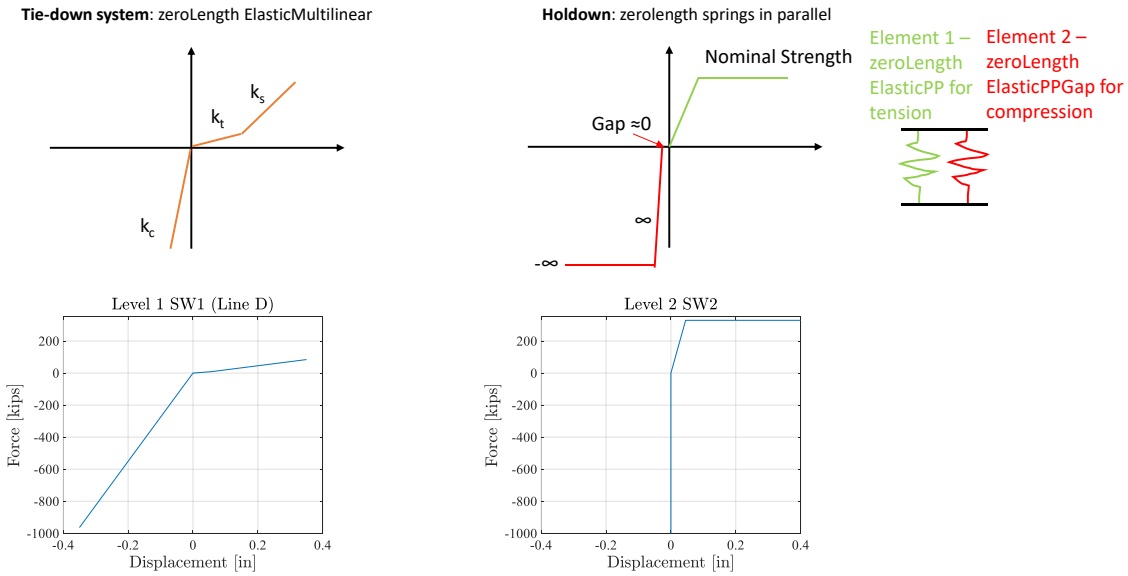

Figure 7. Examples of tie-down system and holdowns properties

2.3. Estimate of dynamic properties: modal analysis vs. eigenvalue analysis

Modal analysis of the numerical model with consideration of stiffness contribution from shear wall springs only was compared with the eigenvalue analysis result from the numerical model. Table 1 summarizes the first 6 modes for each case. Compared with the code-based period, T_a = 0.632 s, a mismatch is observed between the code-based period and the analysis of Table 1, the numerical model and modal analysis suggesting a more flexible behavior of the building. It can be observed that for both cases, the ordering of the first 6 modes is consistent between the modal analysis and eigenvalue analysis. The difference between modal analysis and eigenvalue analysis results is significantly smaller when finishes are consistently considered amongst both models. The impact of finishes in this regard consistently demonstrates a pronounced impact on the fundamental periods.

Table 1. Summary of modal analysis compared with eigenvalue analysis (w/ and w/o finish) for model 1

Finished						**Unfinished**					
Modal analysis			**Eigenvalue analysis**			**Modal analysis**			**Eigenvalue analysis**		
Mode #	**Period [s]**	**Note**	**Mode #**	**Period [s]**	**Note**	**Mode #**	**Period [s]**	**Note**	**Mode #**	**Period [s]**	**Note**
1	0.892	1-T	1	0.739	1-T	1	1.304	1-T	1	0.974	1-T
2	0.844	1-L	2	0.638	1-L	2	1.086	1-L	2	0.719	1-L
3	0.632	1-To	3	0.484	1-To	3	0.865	1-To	3	0.595	1-To
4	0.332	2-T	4	0.276	2-T	4	0.529	2-T	4	0.371	2-T
5	0.323	2-L	5	0.228	2-L	5	0.475	2-L	5	0.265	2-L
6	0.243	2-To	6	0.178	2-To	6	0.370	2-To	6	0.224	2-To

Note: Description, i.e. T: Transverse (N-S direction); L : Longitudinal (E-W direction); To : Torsional

The modal mass participation ratios for the first three predominant modes in each direction are 79/12/4% (L), 85/9/4% (T), and 81/11/4% (To) for modal analysis; 72/10/4% (L), 74/10/3% (T), and 73/9/3% (To) for eigenvalue analysis for the case with finishes. Those are 70/16/8% (L), 83/9/4% (T), and 78/12/4% (To) for modal analysis; 70/11/4% (L), 73/10/3% (T), and 71/10/3% (To) for eigenvalue analysis for the case without finishes.

3. Model 2: Higher fidelity model with refined wall line representation

Previous research on modeling the dynamic response of CFS-framed structures has been mainly dependent on simplifications to reduce computational expenses. Notably, most frequently the shear wall is represented by a nonlinear spring or two diagonal nonlinear braces (Shamim and Rogers 2012); the gravity system is not considered at all (except as a leaning P-D column); and the diaphragms are modeled to be fully-rigid (using a single element). Leng et al. (2017) developed higher-fidelity models for the two-story CFS-NEES test building which could offer a more accurate estimation of the individual CFS-framed components performance under seismic loads; namely assessment of the load path redistribution to chord studs, track, and sheathing which form shear wall lines, for example. Later, Zhang et al. (2022c) developed a high-fidelity model of the lateral response of CFS-framed wall-lines, considering both steel sheet sheathed shear walls and gravity walls, in addition to the effect of non-structural finish. In comparison with simplified models, the higher-fidelity models of both Leng et al. (2017) and Zhang et al. (2022c) showed much higher accuracy in predicting the response of CFS-framed buildings and CFS-framed wall-lines, respectively. In the current study, the high-fidelity model approaches of Leng et al. (2017) and Zhang et al. (2022c) are followed. Model 2 provides the opportunity to understand further the load path redistribution along wall lines and within elements of the SW and GW (chord studs, track, sheathing) - features that are lumped in the aforementioned behavioral consideration.

3.1. Model description

Employing the OpenSeesPy framework (McKenna et al. 2000, Zhu et al. 2018), a higher-fidelity finite element model is constructed. Initially, a finite element model of the test specimen SGGS-1HD from the wall-line dynamic testing program of Singh et al. (2022b, 2022c) is utilized as an example to explain the model (see Figure 8a). In the developed model, displacement-based beam-column line elements are used to represent all framing members (i.e. studs and tracks), as illustrated in Figure 8b. To assign axial and flexural responses separately for the beam-column elements, the “section aggregator” command is utilized. An elastic-perfectly plastic (EPP) material model (scaled to actual nominal capacities) is adopted to simulate the nonlinear axial and flexural response of tracks and field studs. The maximum strength is calculated according to AISI S100-16 (AISI 2016), which accounts for local buckling, distortional buckling, and yielding. For the chord studs, a more complicated nonlinear model is chosen. This chord-stud model uses *Pinching4* material model from OpenSeesPy library (which uses a complete four-point backbone and takes into account unloading stiffness degradation, reloading stiffness degradation, and strength degradation) for both local buckling and distortional buckling per Section 9.8 in ASCE 41-17(ASCE/SEI 2017). As for the global buckling of chord and field studs, it is considered by simulating the studs by multiple beam-column elements over the unbraced length. All elements (except for ledger tracks and end joins) use centerline definitions only. On the other hand, for the ledger (rim) tracks and end joints, their full web height is considered using additional beam elements normal and rigidly connected to the horizontal beam-column element representing the ledger track/end joist itself. This permits the joint between studs and ledger-track/end-joist to transfer moment across the full depth of the ledger/joist as opposed to a single-point joint, and hence offers a potentially more accurate transfer of moment between these elements.

The steel sheet sheathing in Figure 8a is modeled using two diagonal truss elements (Figure 8b) employing a *Pinching4* material model, whose parameters are calibrated depending on the cyclic test data of independent CFS-framed shear wall with steel sheathing (Rizk and Rogers 2017). Shear wall specimen CW2, from Rizk and Rogers (2017), is chosen as it has the closest configuration (similar framing thickness, sheathing thickness, and fastener spacing) compared with the SGGS-1HD wall-line test. The difference in heights between CW2 specimen (2.44 m or 8 ft) and SGGS-1HD (2.74 m or 9 ft) is also taken into consideration in the material model of the sheathing. In the case of walls with nonstructural finishes, additional diagonal truss elements employing *Pinching4* hysteretic model are assigned. The parameters of the *Pinching4* material model of gypsum finish are defined based on cyclic tests of CFS-framed walls with only gypsum boards (Morello 2009).

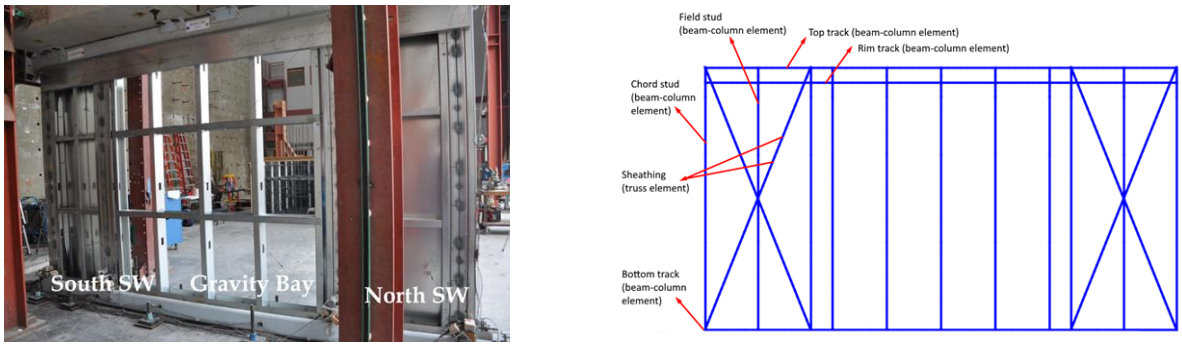

(a) (b)

Figure 8. (a) Quasi-static test specimen SGGS-1HD performed by Singh et al. (2022b, 2022c); (b) OpenSeesPy finite element model of SGGS-1HD wall-line specimen

3.2. Model validation

The performance of the constructed finite element model is evaluated by comparing with the data obtained from the SGGS-1HD wall line test. As shown in Figure 9a, there is a very good agreement between the predicted and experimental cyclic responses. Figures 9b and 9c further illustrate the finite-element axial force and bending moment diagrams of the wall line. At the time of preparation of this paper, the presented high-fidelity wall-line model is being advanced and validated within various multi-story wall-lines and multi-story CFS-framed buildings. Some initial results of these advanced models are presented in Figures 10 and 11.

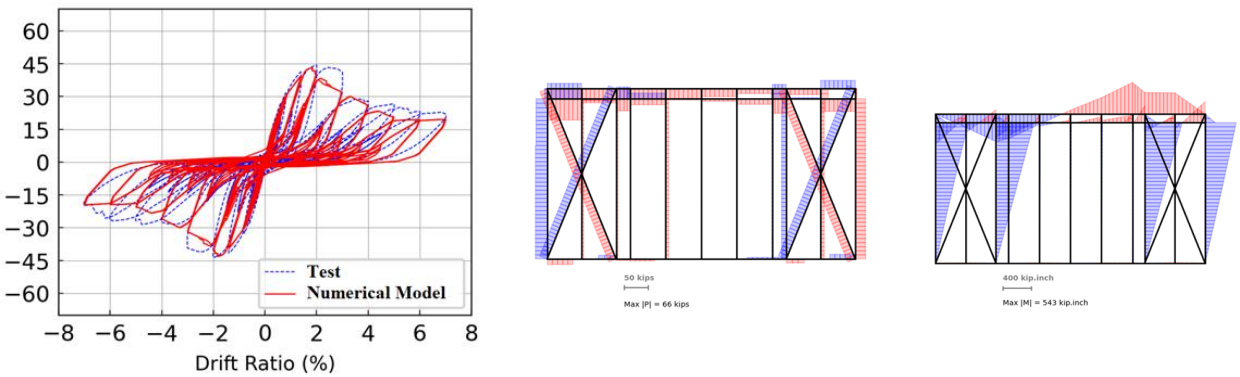

(a) (b) (c)

Figure 9. (a) Comparison of experimental and numerical base-shear vs. drift ratio response of SGGS-1HD); Finite element (b) axial force diagram and (c) bending moment diagram (at maximum load)

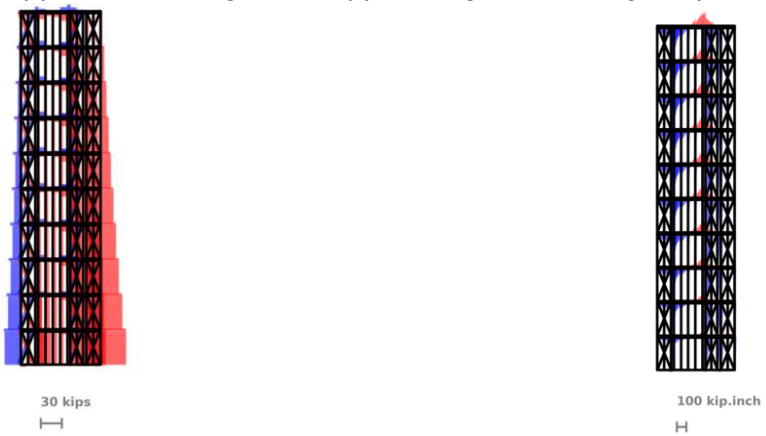

(a) (b)

Figure 10. Finite element (a) axial force diagram and (b) bending moment diagram of a multi-story wall-line

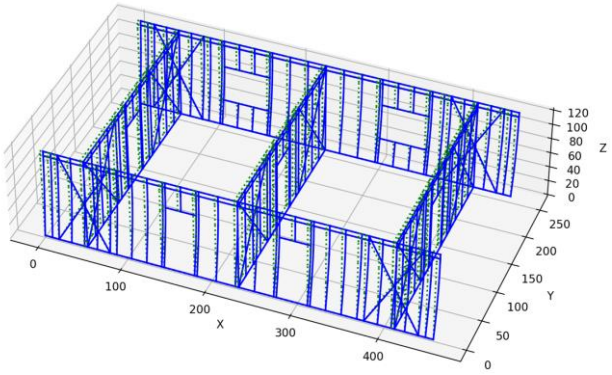

Figure 11. Finite element deformed shape of 1-story CFS-framed building under unidirectional pushover analysis.

4. Discussion on pros and cons of both models

Model 1 utilizes a simplistic strategy that boasts efficiency in computing by minimizing model degrees-of-freedom, assuming rigid diaphragms, lumped masses, and uniaxial spring elements to capture the lumped behaviors of the lateral load-resisting shear walls, gravity walls, and tie-down systems. This design-level phenomenological-based model can provide a significantly fast computational turnaround time, while effectively capturing the dynamic characteristics. The limited computational overhead makes this model a useful tool for conducting extensive suites of earthquake motion analyses. The model continues to be refined and calibrated using the shake table test data and may also be useful for incremental dynamic analysis and parametric studies. However, due to the modeling approach, the vertical load might not be fully captured since only a limited number of vertical force-resisting components are incorporated and therefore only a portion of the gravity load can be assigned, resulting in a possible limitation in response history analyses when vertical ground motion inputs are considered.

Model 2 boasts higher fidelity, though requires parallel computing to enhance the computational speed, with wall lines captured with a suite of discrete beam and truss elements and interconnecting springs at boundary and other connections to capture local behaviors induced along the lateral force-resisting system and associated boundaries. Due to the complex nature of this modeling approach, an extensive amount of calibration for material properties employed in the model is needed in addition to the significant computational overhead that this model requires. Assembling the 2D wall lines into a 3D model can also be challenging. Currently, for a 2D wall line pushover, the required computational time is already substantial even with parallel computing, therefore significantly longer running time will be expected when performing response history analyses.

5. Summary and future steps

The system-level benchmark test of the CFS-NHERI 10-story building at the newly upgraded LHPOST6 at NHERI@ UC San Diego Experimental Facility will provide a unique opportunity to evaluate the earthquake and post-earthquake fire performance of tall CFS-framed buildings under multi-directional earthquake excitation. In preparation for this test program, two FE models are developed and are introduced in this paper. Nonlinear static analyses will be performed to obtain the shear distribution profile of the test building after continuous development and comprehensive material properties calibration. These models will then be used to predict the dynamic characteristics and subsequently to simulate the nonlinear dynamic behavior of the designed specimen under different earthquake motions. Predictions from these numerical models will be cross-compared and used to support selection and scaling of ground motions during the full-scale shake table program.

6. Acknowledgements

The research presented is funded through the National Science Foundation (NSF) grants CMMI 1663569 and CMMI 1663348, project entitled: Collaborative Research: Seismic Resiliency of Repetitively Framed Mid-Rise Cold-Formed Steel Buildings. Support for the first author from the Structural Engineering Distinguished Fellowship provided by the Department of Structural Engineering at University of California San Diego is

greatly appreciated. Findings, opinions, and conclusions are those of the authors and do not necessarily reflect those of the sponsoring organizations.

7. References

AISI (2015a). *North American Specification for Cold-Formed Steel Structural Framing, AISI S240-15*. American Iron and Steel Institute, Washington, D.C., USA.

AISI (2015b). *North American Specification for Seismic Design of Cold-Formed Steel Structural Systems, AISI S400-15*. American Iron and Steel Institute, Washington, D.C., USA.

AISI (2016). *North American Specification for the Design of Cold-Formed Steel Structural Members, AISI S100-16*. American Iron and Steel Institute, Washington, D.C., USA.

ASCE/SEI (2016). *Minimum Design Loads and Associated Criteria for Buildings and Other Structures, ASCE/SEI 7-16*. American Society of Civil Engineers, Reston, VA, USA.

ASCE/SEI (2017). *Seismic Evaluation and Retrofit of Existing Buildings, ASCE/SEI 41-17*. American Society of Civil Engineers, Reston, VA, USA.

ASCE/SEI (2022). *Minimum Design Loads and Associated Criteria for Buildings and Other Structures, ASCE/SEI 7-22*. American Society of Civil Engineers, Reston, VA, USA.

Castaneda, H. (2022). *Seismic performance of cold-formed steel diaphragms*. Ph.D. thesis. University of Massachusetts, Amherst, Amherst, MA, USA.

Campiche, A., Fiorino, L., and Landolfo, R. (2020). Numerical modelling of CFS two-storey sheathing-braced building under shaking-table excitations. *Journal of Constructional Steel Research*, 170: 106110. DOI: https://doi.org/10.1016/j.jcsr.2020.106110.

ClarkDietrich. (2023). *ClarkDietrich Holdown Design Loads*. https://clarkdietrich.com.

Folz, B. and Filiatrault, A. (2004a). Seismic analysis of woodframe structures. I: Model formulation. *Journal of Structural Engineering*, 130(9): 1353–1360. DOI: https://doi.org/10.1061/(ASCE)0733-9445(2004)130:9(1353).

Folz, B. and Filiatrault, A. (2004b). Seismic analysis of woodframe structures. II: Model implementation and verification. *Journal of Structural Engineering*, 130(9): 1361–1370. DOI: https://doi.org/10.1061/(ASCE)0733-9445(2004)130:9(1361).

Franklin, N. P., Ahmed, A., Teh, L. H., Heffernan, E. E., and McCarthy, T. J. (2019). Efficient 3D lateral analysis of cold-formed steel buildings. *Journal of Constructional Steel Research*, 160: 16-22. DOI: https://doi.org/10.1016/j.jcsr.2019.05.029.

Hutchinson, T. C., Wang, X., Hegemier, G., Kamath, P., and Meacham, B. (2021). Earthquake and postearthquake fire testing of a midrise cold-formed steel-framed building. I: Building response and physical damage. *Journal of Structural Engineering*, 147(9): 04021125. DOI: https://doi.org/10.1061/(ASCE)ST.1943-541X.00030.

Leng, J., Peterman, K. D., Bian, G., Buonopane, S. G., and Schafer, B. W. (2017). Modeling seismic response of a full-scale cold-formed steel-framed building. *Engineering Structures*, 153: 146-165. DOI: https://doi.org/10.1016/j.engstruct.2017.10.008.

Lowes, L. N., Mitra, N., and Altoontash, A. (2003). *A beam-column joint model for simulating the earthquake response of reinforced concrete frames*. PEER Report 2003-10. Pacific Earthquake Engineering Research Center, University of California, Berkeley, CA, USA.

McKenna, F., Fenves, G. L., and Scott, M. H. (2000). *Open System for Earthquake Engineering Simulation*, http://opensees.berkeley.edu. University of California, Berkeley.

Morello, D. (2009). *Seismic performance of multi-storey structures with cold-formed steel wood sheathed shear walls*. Master Thesis. Department of Civil Engineering and Applied Mechanics, McGill University, Montreal, Canada.

Peterman, K. D., Stehman, M. J. J., Madsen, R. L., Buonopane, S. G., Nakata, N., and Schafer, B. W. (2016). Experimental seismic response of a full-scale cold-formed steel-framed building. I: System-level response. *Journal of Structural Engineering*, 142(12): 04016127. DOI: https://doi.org/10.1061/(ASCE)ST.1943-541X.0001577.

Rizk, R. and Rogers, C.A. (2017). *Higher strength cold-formed steel framed steel shear walls for mid-rise construction*. Research Report, Department of Civil Engineering and Applied Mechanics, McGill University, Montreal, Canada.

Shamim, I. and Rogers, C. A. (2012). Numerical modeling and calibration of CFS framed shear walls under dynamic loading. *Proceedings of the 21st International Specialty Conference on Cold-Formed Steel Structures*, St. Louis, MO, USA.

Singh, A., Hutchinson, T. C., Torabian, S., Schafer, B. W., Peterman, K. D., Padgett, L., and Jones, H. (2022a). Structural design narrative of the CFS-NHERI 10-story test building for multi-dimensional shake table testing. *Proceedings of the Cold-Formed Steel Research Consortium Colloquium 2022*, Baltimore, MD, USA.

Singh, A., Hutchinson, T. C., Wang, X., Zhang, Z., Schafer, B. W., Derveni, F., Castaneda, H., and Peterman K. D. (2022b). Steel Sheet Sheathed Cold-formed Steel Framed In-line Wall Systems. I: Impact of Structural Detailing. *Journal of Structural Engineering*, 148(12): 04022193. DOI: https://doi.org/10.1061/(ASCE)ST.1943-541X.0003433.

Singh, A., Hutchinson, T. C., Wang, X., Zhang, Z., Schafer, B. W., Derveni, F., Castaneda, H., and Peterman K. D. (2022c). Steel Sheet Sheathed Cold-Formed Steel Framed In-line Wall Systems. II: Impact of Nonstructural Detailing. *Journal of Structural Engineering*, 148(12): 04022194. DOI: https://doi.org/10.1061/(ASCE)ST.1943-541X.0003434.

Singh, A. (2023). *Seismic Behavior of Cold-Formed Steel-Framed Wall-Line Systems in Mid-Rise Buildings*. Doctoral dissertation. University of California San Diego, La Jolla, CA.

Singh, A., Zhang, J., Rivera, D., Eladly, M., Jones, H., Kovac, A., Padgett, L., Rivera, D., Smith, K., Torabian, S., Peterman, K., Schafer, B., and Hutchinson, T. (2024). CFS-NHERI 10-Story Building Shake Table Test Specimen: Design Updates. *Proceedings of the 18th World Conference on Earthquake Engineering (WCEE2024)*, Milan, Italy.

UC San Diego. (2023). *CFS-NHERI: 10-Story Building Capstone Test Program*. Accessible at: https://cfs10.ucsd.edu.

van de Lindt, J. W., Pei, S., Liu, H., and Filiatrault, A. (2010). Three-dimensional seismic response of a full-scale light-frame wood building: Numerical study. *Journal of Structural Engineering*, 136(1): 56–65. DOI: https://doi.org/10.1061/(ASCE)ST.1943-541X.000008.

Van Den Einde, L., Conte, J. P., Restrepo, J. I., et al. (2021). NHERI@UC San Diego 6-DOF large high-performance outdoor shake table facility. *Frontiers in Built Environment*, 6. DOI: https://doi.org/10.3389/fbuil.2020.580333.

Zhang, Z., Singh, A., Dervani, F., Torabian, S., Peterman, K. D., Hutchinson, T. C., and Schafer, B. W. (2021). Cyclic experiments on isolated steel sheet connections for CFS framed steel sheet sheathed shear walls with new configurations. *Engineering Structures*, 244: 112805. DOI: https://doi.org/10.1016/j.engstruct.2021.112805.

Zhang, Z., Eladly, M., Rogers, C., and Schafer B. W. (2022a). Cold-Formed Steel Framed Shear Wall Database. In *CFS-NHERI: Seismic Resiliency of Repetitively Framed Mid-Rise Cold-Formed Steel Buildings*. DesignSafe-CI. DOI : https://doi.org/10.17603/ds2-ag1e-6m27.

Zhang, Z., Singh, A., Dervani, F., Torabian, S., Peterman, K. D., Hutchinson, T. C., and Schafer, B. W. (2022b). Cyclic experiments on steel sheet connections for standard CFS framed steel sheet sheathed shear walls. *Journal of Structural Engineering*, 148(2): 04021261. DOI: https://doi.org/10.1061/(ASCE)ST.1943-541X.000323.

Zhang, Z., Speicher, M. S., Singh, A., Hutchinson, T. C., and Schafer, B. W. (2022c). Effects of Modeling Decisions on the Lateral Performance of Cold-Formed Steel Framed Walls. *Proceedings of the Cold-Formed Steel Research Consortium Colloquium 2022*, Baltimore, MD, USA.

Zhang, Z. (2023). *Simulation and Performance of Steel Sheet Sheathed Shear Walls in CFS-Framed Building Systems*. Doctoral dissertation. Johns Hopkins University, Baltimore, MD, USA.

Zhu, M., McKenna, F., and Scott, M. H. (2018). OpenSeesPy: Python library for the OpenSees finite element framework. *Software X*, 7: 6-11. DOI: https://doi.org/10.1016/j.softx.2017.10.009.